DMD Fast Forward. Published on December 3, 2021 as DOI: 10.1124/dmd.121.000582
This article has not been copyedited and formatted. The final version may differ from this version.

Mechanistic study on the species differences in excretion pathway of HR011303 in human and rats

Zitao Guo[a,b,1], Mengling Liu[b,c,1], Jian Meng[b], Yaru Xue[b], Qi Huang[d], Yuandong Zheng[b], Yali Wu[b,c], Zhendong Chen[b], Jinghua Yu[b], Dafang Zhong[b,c], Guangze Li[d], Xiaoyan Chen[a,b,c] and Xingxing Diao[b,c]*

[a]*Shanghai University, Shanghai 200444, China.*

[b]*Shanghai Institute of Materia Medica, Chinese Academy of Sciences, Shanghai 201210, China.*

[c]*University of Chinese Academy of Sciences, Beijing 100049, China*

[d]*Jiangsu Hengrui Medicine Co. Ltd. Lianyungang, Jiangsu 450000, China*

*Corresponding author:

Xingxing Diao, E-mail: xxdiao@simm.ac.cn

[1]Contributed equally to this work.

DMD Fast Forward. Published on December 3, 2021 as DOI: 10.1124/dmd.121.000582
This article has not been copyedited and formatted. The final version may differ from this version.

Running title: HR011303 excretion species differences

Address correspondence to:

Xingxing Diao, Shanghai Institute of Materia Medica, Chinese Academy of Sciences, Shanghai 201210, China

E-mail address: xxdiao@simm.ac.cn

Number of text pages: 44

Number of tables: 1

Number of figures: 11

Number of references: 42

Number of words in the Abstract: 250

Number of words in the Introduction: 624

Number of words in the Discussion: 1286

DMD Fast Forward. Published on December 3, 2021 as DOI: 10.1124/dmd.121.000582
This article has not been copyedited and formatted. The final version may differ from this version.

Abbreviations:

BCRP, breast cancer resistance protein; CE, collision energy; CL_{bile}, biliary clearance; HEK, human embryonic kidney; LC-MS/MS, liquid chromatography/tandem mass spectrometry; HPLC, high performance liquid chromatography; MRP, multidrug resistance-associated protein; MS, mass spectrometry; OAT, organic anion transporter; OATP, organic anion-transporting polypeptide; P-gp, P-glycoprotein; RKMs, rat kidney microsomes; RLMs, rat liver microsomes; SCRH, sandwich-cultured rat hepatocytes; SCHH, sandwich-cultured human hepatocytes; SD, Sprague-Dawley; UGT, UDP-glucuronosyltransferase; URAT1, urate transporter 1.

DMD Fast Forward. Published on December 3, 2021 as DOI: 10.1124/dmd.121.000582
This article has not been copyedited and formatted. The final version may differ from this version.

Abstract

Excretion of [^{14}C]HR011303-derived radioactivity showed significant species difference. Urine (81.50% of dose) was the main excretion route in healthy male subjects, whereas feces (87.16% of dose) was the main excretion route in rats. To further elucidate the underlying cause for excretion species differences of HR011303, studies were conducted to uncover its metabolism and excretion mechanism. M5, a glucuronide metabolite of HR011303, is the main metabolite in humans and rats. Results of rat microsomes incubation study suggested that HR011303 was metabolized to M5 in the rat liver. According to previous studies, M5 is produced in both human liver and kidney microsomes. We found M5 in human liver can be transported to the blood by multidrug resistance-associated protein (MRP) 3 and then the majority of M5 can be hydrolyzed to HR011303. HR011303 enters the human kidney or liver through passive diffusion, whereas M5 is taken up through organic anion transporter (OAT) 3, organic anion-transporting polypeptide (OATP) 1B1, and OATP1B3. When HR011303 alone was present, it can be metabolized to M5 in both sandwich-cultured rat hepatocytes (SCRH) and sandwich-cultured human hepatocytes (SCHH) and excreted into bile as M5 in SCRH. Using transporter inhibitors in sandwich-cultured model and membrane vesicles that expressing MRP2 or Mrp2, we found M5 was substance of MRP2/Mrp2 and the bile efflux of M5 mainly mediated by MRP2/Mrp2. Considering the significant role of MRP3/Mrp3 and MRP2/Mrp2 in the excretion of glucuronides, the competition between them for M5 was possibly the determinant for the different excretion routes in humans and rats.

DMD Fast Forward. Published on December 3, 2021 as DOI: 10.1124/dmd.121.000582
This article has not been copyedited and formatted. The final version may differ from this version.

Significance Statement

Animal experiments are necessary to predict dosage and safety of candidate drugs prior to clinical trials. However, extrapolation results often differ from actual situation. For HR011303, excretory pathways exhibited a complete reversal, through urine in humans and feces in rats. Such phenomena have been observed in several drugs, but no in-depth studies have been conducted to date. In the present study, the excretion species differences of HR011303 can be explained by the competition for M5 between MRP2/Mrp2 and MRP3/Mrp3.

DMD Fast Forward. Published on December 3, 2021 as DOI: 10.1124/dmd.121.000582
This article has not been copyedited and formatted. The final version may differ from this version.

Introduction

Animal experiments are needed prior to the clinical trials of candidate drugs to predict dosage, safety, and toxicity. Rats are the most commonly used animal models (Takano et al., 2010). However, due to obvious species differences in the types and expression levels of metabolizing enzymes (Shiratani et al., 2008; Stringer et al., 2009; Mazur et al., 2010) and transporters (Hillgren et al., 2013; Wang et al., 2015), the extrapolated results often differed from the actual results (Lin et al., 1996). Direct extrapolation of biliary clearance (CL_{bile}) from preclinical small animals sometimes leads to an overestimation of human CL_{bile}. For example, an overestimation by 400- and 150-fold was observed for cefamandole and vincristine, respectively (Ratzan et al., 1978; Ansede et al., 2010; Grime and Paine, 2013).

Transporters play an important role in the distribution and elimination of drugs (Tu et al., 2013; Ma et al., 2014; Nigam and Sanjay, 2015). MRP3 is located at the basolateral membrane and mediates the efflux of substrates, particularly glucuronides and glutathione conjugates, into sinusoidal blood. By contrast, OATPs are the major drug uptake transporters in hepatocytes (Hillgren et al., 2013). Breast cancer resistance protein (BCRP), P-glycoprotein (P-gp), and MRP2 are localized to the canalicular membrane of hepatocytes and mediate the export of xenobiotics into bile (Robertson and Rankin, 2006; Konig et al., 2013). MRP2/Mrp2 and MRP3/Mrp3 possibly play a decisive role in glucuronides excretion. Mrp2 and Mrp3 provide alternative routes for the hepatic excretion of morphine-glucuronides (Van De Wetering et al., 2007). Mrp2 plays an important role in doxorubicin elimination. The levels of Mrp3 (Abcc3) in liver of $Mrp2^{-/-}$ mice increase by approximately 2-fold (Nezasa et al., 2006; Vlaming et al.,

2006). The upregulation of basolateral MRP3/Mrp3 compensates for the reduced ability of MRP2/Mrp2 (Chandra et al., 2005).

HR011303 is a highly selective urate transporter 1 (URAT1) inhibitor, which is clinically intended to treat gout. It is currently in phase III clinical trials in China (Peng et al., 2016; Wang et al., 2019). When comparing mass balance results in humans and rats, significantly different excretion routes were observed in these two species. Early animal studies showed that after intragastric administration of [^{14}C]HR011303 in Sprague-Dawley (SD) rats, drug-related substances mainly effluxed into bile and excreted in the feces. The recovery rate of radioactivity was 87.20% in the feces and 10.10% in the urine within 0-168 h (Fig. 1A). The recovery rate was 70.90% in the bile within 0-48 h (Fig. 1B). In contrast, in healthy male Chinese subjects, urine was the main excretion route after oral administration of [^{14}C]HR011303. Within 0-216 h, 81.50% of the recovered drug-related substances were excreted in the urine, and 10.26% were excreted in the feces (Fig. 1C). The main metabolite in human urine and rat bile was the glucuronide metabolite M5. The in vitro microsome incubation results showed that HR011303 could be metabolized to M5 in human liver microsomes (HLMs) and human kidney microsomes (HKMs) (companion manuscript, DMD-AR-2021-000581). In this study, we explored the underlying reasons for the species differences in the excretion of HR011303 from the perspective of transporters. We aimed to reveal the mechanisms underlying such excretion differences. Results will serve as evidence for similar situations that may arise new drug the development.

The huge differences in HR011303 excretion between humans and rats inspired a series of experiments that aimed to uncover HR011303's disposition and excretion process in rats and humans. Experiments were performed to achieve the following objectives: 1) to identify the main metabolic sites of HR011303 in rats; 2) to characterize the role of MRP3 in the distribution

process of HR011303 and M5; 3) to identify the transporters involved in HR011303 and M5 kidney and hepatic uptake; and 4) to investigate the HR011303 and M5 bile efflux in rat and human hepatocytes.

Materials and Methods

Chemicals and reagents. HR011303 (98.40% purity), M5 (95.40% purity), and internal standard (IS) SHR144764 (98.20% purity) were kindly supplied by Jiangsu Hengrui Medicine Co., Ltd. (Lianyungang, China). High-performance liquid chromatography (HPLC)-grade acetonitrile and methanol were purchased from Sigma (St. Louis, MO, USA). Dimethyl sulfoxide was obtained from Sinopharm Chemical Reagent Co., Ltd. (Shanghai, China). Formic acid was purchased from Rhawn Chemical Reagent Co., Ltd. (Shanghai, China). Sodium carboxymethyl cellulose (CMC-Na) was provided by Aladdin (Shanghai, China). The following were purchased from Meilunbio (Dalian, China): uridine 5′-diphosphoglucuronic acid (UDPGA), protease inhibitor cocktail, alamethicin, 3-(N-morpholino) propanesulfonic acid (MOPS), adenosine 5'-triphosphate disodium salt (Na_2ATP), adenosine 5′-monophosphate disodium salt (Na_2AMP), magnesium chloride, Hanks' buffered salt solution (HBSS), and D-Hanks. Other commercially available reagents used in the experiments were of analytical grade.

Pooled male SD rat liver microsomes (RLMs) were supplied by Corning Gentest (Woburn, MA, USA). Pooled male SD rat kidney microsomes (RKMs) were purchased from XenoTech, Inc. (Lenexa, KS, USA). Inside-out Sf9 insect cell membrane vesicles that expressing MRP2, Mrp2 and MRP 3 were provided by GenoMembrane Co., Ltd. (Yokohama, Japan). Blank human plasma was kindly supplied by the People's Hospital of Weifang High-tech Industrial Development Zone (Weifang, China). Cryopreserved human hepatocytes were purchased from IVT (Baltimore, MD, USA). OATP1B1-, OATP1B3-, OAT1-, OAT3-, or organic cation

transporter 2 (OCT2)-expressing human embryonic kidney 293 (HEK293) cell lines and empty-vector-transfected control cells were constructed at HD Biosciences Co., Ltd. (Shanghai, China).

Sprague-Dawley rats were obtained from Jiesijie laboratory animal Co., Ltd (Shanghai, China). The study was approved by the Animal Ethics Committee of Shanghai Institute of Materia Medica, Chinese Academy of Sciences. Rats were housed and handled according to the Guidelines for Care and Use of Laboratory Animals at Shanghai Institute of Materia Medica, Chinese Academy of Sciences.

Rats mass balance study [^{14}C]HR011303 and HR011303 sodium salts were dissolved in 0.5% CMC-Na for mass balance study in rats, and the concentration for oral administration was 8.95 mg/kg (81.9 μCi/kg). The following samples were collected: pre-dose urine and fecal samples; urine samples at 0–8, 8–24, 24–48, 48–72, 72–96, 96–120, 120–144, and 144–168 h post-dose; and feces samples at 0–24, 24–48, 48–72, 72–96, 96–120, 120–144, and 144–168 h post-dose (3 male and 3 female rats, respectively). Bile sample were collected pre-dose and at 0–4, 4–8, 8–24, and 24–48 h after administration (3 male and 3 female rats).

For urine and bile samples, a liquid scintillation counter (LSC) (Tri-Carb 3110TR, PerkinElmer, Waltham, MA, USA) was used to measure the radioactivity after adding an appropriate amount of urine or bile to 5 mL scintillation fluid. While feces were mixed with 3 times weigh of acetonitrile–water (1:1, *v*/*v*) and then homogenized. About 300 mg homogenate was combusted using an OX-501 Biological Oxidizer (Harvey, Tappan, NY, USA) and the generated $^{14}CO_2$ was captured by alkaline RDC liquid scintillation cocktail. Finally, the radioactivity was measured with a Tri-Carb 3110TR liquid scintillation counter.

In vitro incubations of HR011303 with pooled RLMs and RKMs. HR011303 was dissolved in methanol-water (50:50, *v*/*v*) to prepare a 2 mM stock solution. Alamethicin was dissolved in dimethyl sulfoxide (DMSO) to prepare a stock solution with a concentration of 40 mg/mL, which was then diluted to obtain a working solution with 50 mM Tris-HCl buffer (8 mM $MgCl_2$, pH 7.5). After incubation at 37°C for 3 min, UDPGA was added to initiate the reaction. The final incubation system was 200 μL and included 50 mM Tris-HCl buffer, 8 mM magnesium chloride, 25 μg/mL of alamethicin, 5 μM HR011303, RLMs or RKMs (1 mg protein/mL), and 2 mM UDPGA. After incubation at 37°C for 1 h, the reaction was terminated by adding 200 μL of cold acetonitrile. An incubation system without microsomes was used as the negative control.

Efflux transporter MRP3 study. The efflux of HR011303 and M5 was evaluated in human MRP3-expressing membrane vesicles. In transport assays, a modified rapid filtration technique was used based on the manufacturer's protocol (GenoMembrane Co). Membrane vesicles (50 μg of protein) and test compounds were incubated with or without ATP (5 mM) in the transport medium (50 μL, pH 7.4), which contained 50 mM MOPS-Tris, and 10 mM $MgCl_2$. The process was terminated after 10 min of incubation by adding 200 μL ice-cold quenching solution (40 mM MOPS-Tris and 70 mM KCl). The incubation mixture was quickly transferred to a Millipore 96-well glass fiber filter plate (Millipore, MA, USA) and washed twice with ice-cold quenching solution. The compound trapped in the membrane vesicles was retained on the filters and released by adding 200 μL of ethanol-water (50:50, *v*/*v*). The compounds inside the vesicles were analyzed by liquid chromatography/tandem mass spectrometry (LC-MS/MS). ATP-dependent transport was evaluated according to the ratio of transport with ATP to that without ATP (Gao et al., 2012).

DMD Fast Forward. Published on December 3, 2021 as DOI: 10.1124/dmd.121.000582
This article has not been copyedited and formatted. The final version may differ from this version.

Transporter-transfected cell culture. Transporter-transfected cells were cultured as previously reported (Takeuchi et al., 2015). HEK293 cells were cultured in Dulbecco's modified Eagle's medium supplemented with 10% fetal bovine serum, 2 mM L-glutamine, 1% modified Eagle's medium nonessential amino acid, 100 μg/mL of penicillin, and 100 μg/mL of streptomycin. Cultures were maintained in a humidified atmosphere containing 5% CO_2 at 37°C.

Uptake transporters study. Uptake of HR011303 and M5 was evaluated using HEK-OATP1B1, HEK-OATP1B3, HEK-OAT1, HEK-OAT3 and HEK-mock cell lines according to a previously reported method (Han et al., 2010). Transfected HEK293 and mock control cells were seeded on BioCoat poly-D-lysine-coated 24-well plates (BD Biosciences) at a density of 3.0×10^5 cells/well. After 36 h of culture, the cells were washed twice and equilibrated in prewarmed Hank's balanced salt solution (HBSS) for 10 min. The uptake was initiated by adding 0.5 mL HBSS containing test compounds or a mixed solution of the test drug and transporter inhibitor to the corresponding cell wells. Then, the uptake was terminated at a designated time by discarding the medium and washing the cells twice with ice-cold HBSS. Cells were lysed with methanol-water (70:30, *v*/*v*). The test compound concentrations of the were determined by LC-MS/MS. Total cellular protein levels were measured using a BCA protein assay kit. The main kinetic parameters were calculated using Prism 8 (GraphPad Software, Inc., San Diego, CA).

Stability of M5 in human plasma. Stock solution (10 mM) was prepared by dissolving an appropriate amount of M5 in DMSO and was diluted to 50 μM with PBS. The incubation mixtures (100 μL of total volume) consisted of 90 μL of human plasma (5% volume of cocktail inhibitor or DMSO) and 10 μL of the M5 solution. The final incubation concentration of M5 was 5 μM. The reactions were maintained at 37 °C for 0, 5, 10, 20, and 40 min and terminated with 1000 μL of ice-cold acetonitrile (0.1%FA, IS:100 ng/mL). Each incubation was conducted in

duplicate. M5 concentration was quantified by using LC-MS/MS. The results are expressed as the percentage of the remaining M5 (Jiang et al., 2016).

Preparation and sandwich-culture of human and rat primary hepatocytes. Cryopreserved human hepatocytes were thawed according to the manufacturer's instructions (Baltimore, MD, USA). Rat hepatocytes were isolated from male SD rats using a reported previously two-step recirculating collagenase perfusion (Xue et al., 2020). Cells were suspended at approximately 7×10^5 cells/mL in a plating medium and then added at approximately 0.5 mL per well to 24-well plates pretreated with rat tail collagen. After 4 h of incubation at 37℃ and 5% carbon dioxide, the cells were overlaid with 0.25 mg/mL of Type I Matrigel solution prepared in a feeding medium. The medium was replaced every 24 h. Studies were conducted on day 5 for SCRH and day 6 for SCHH.

Hepatobiliary efflux of HR011303 SCRHs were used to investigate the bile efflux of HR011303 in rats. Different transporter inhibitors were used to investigate the contribution of different transporters to the efflux process (Shen et al., 2012). Hepatocytes were washed thrice with 400 μL of either HBSS containing calcium (standard buffer) or Hank's balanced salt solution without calcium (calcium-free buffer) and incubated with the third wash solution either in the presence or absence of transporter inhibitors (Verapamil for MDR1 (P-gp)/Mdr1, Novobiocin for BCRP/Bcrp, MK571 for MRP2/Mrp2) for 10 min at 37°C. The wash solution was removed. Then, the cells were incubated with the test drug solution or a mixed solution of the test drug and transporter inhibitor according to the experimental design at 37°C for 15 min. The medium was discarded after the incubation. Cells were rinsed with ice-cold HBSS thrice, and the cell samples were stored at -80℃ for analysis. After the repeated freezing and thawing of the cells, the total amount of HR011303 or M5 in hepatocytes plus bile (standard HBSS) and

DMD Fast Forward. Published on December 3, 2021 as DOI: 10.1124/dmd.121.000582
This article has not been copyedited and formatted. The final version may differ from this version.

hepatocytes (Ca^{2+}-free HBSS) was determined by LC-MS/MS. Total cellular protein levels were measured using a BCA protein assay kit.

The bile excretion index (BEI) represents the fraction of the analyte excreted into the bile pockets (Chandra and Brouwer, 2004). A BEI value greater than 10% indicated that the compound was considered to be excreted through the bile (Pan et al., 2012). The BEI value was calculated using to the following equation:

$$\mathrm{BEI} = \frac{A_{cells+bile} - A_{cells}}{A_{cells+bile}} \times 100$$

where $A_{cells+bile}$ and A_{cells} are the accumulation of compounds in sandwich-cultured hepatocytes measured in the presence and absence of Ca^{2+}.

Efflux transporter MRP2/Mrp2 study. To further evaluate the involvement of MRP2 or Mrp2 in the efflux of HR011303 and M5, human MRP2 and rat Mrp2-expressing membrane vesicles were used. The experimental operation was the same as the "Efflux transporter MRP3 study."

Analytical conditions. The analysis method used for microsome incubation was the same as that used in Zheng's manuscript (companion manuscript, DMD-AR-2021-000581). For LC-MS/MS quantitative analysis, separation of analytes from the matrix was achieved via an Agilent 1290 UHPLC system (Agilent, Santa Clara, CA, USA) on an HSS T3 column with temperature maintained at 40°C. MS detection was conducted by an Agilent 6495 triple-quadrupole mass spectrometer (Agilent). Multiple reaction monitoring fragmentation transitions of *m/z* 338.1→240.0 (HR011303), *m/z* 514.1→338.2 (M5) and *m/z* 328.1→230.0 (IS) were monitored

in positive electrospray ionization mode (Wang et al., 2019). The mobile phase consisted of a mixture of 0.1% formic acid in water (A) and 0.1% formic acid in acetonitrile (B). The flow rate was set to 0.3 mL/min. Gradient elution was initiated at 35% B, maintained for 0.5 min, and increased to 95% B linearly in 0.9 min and maintained for 1.1 min. The elution was finally decreased to 35% B to re-equilibrate the column for 0.9 min. The mass spectrometer parameters were as follows: capillary voltage, +3.0 kV; nozzle voltage, +1.5 kV; nebulizer gas pressure, 30 psi; carrier gas, 14 mL/min and 250°C; and sheath gas, 11 mL/min and 300°C.

DMD Fast Forward. Published on December 3, 2021 as DOI: 10.1124/dmd.121.000582
This article has not been copyedited and formatted. The final version may differ from this version.

Results

Mass balance in rats. Fecal excretion was the predominant route of elimination constituting 87.20% of the administered dose. In contrast, urine excretion accounted for 10.10% of the administered dose, as shown in Fig. 1A. Radioactivity recovery in bile was 70.90% (Fig.1B).

Metabolism of HR011303 in pooled RLMs and RKMs. To study the metabolic sites of HR011303 in rats, incubation was performed with RLMs and RKMs in the presence of UDPGA. The target peak was determined by comparing the retention time and the major product ions with the standard. Fig. 3 shows that unlike in human microsomes, M5 was formed only in RLMs. M5 formation was not observed in the RKMs.

Efflux transporter MRP3 study. M5 is the predominant metabolite in human liver. Thus, MRP3-expressing membrane vesicles were used to determine the interaction between transporters MRP3 and HR011303 as well as M5. As shown in Fig. 4, the ratios of ATP-dependent uptake to nonspecific adsorption (+ATP/-ATP ratio) of M5 were 9.96 (1 μM) and 6.33 (10 μM), whereas the ratios of HR011303 were 0.84 (0.5 μM) and 0.91 (2 μM). No significant ATP-dependent transport was observed in HR011303. M5 rather than HR011303 was a substrate of MRP3, which indicated that M5 produced in human hepatocytes was transported into the blood by MRP3.

Uptake transporter study. HEK293 cells expressing OATP1B1, OATP1B3, OAT1, OAT3, and OCT2 were used to identify transporters that mediated the uptake of HR011303 and M5. In mock cells, the uptake rates of HR011303 were 27.80 and 2.47 pmol/min/mg protein (10 and 2 μM, respectively). The difference in uptake rates between transfected and mock cells of HR011303 was not significant, and transporter inhibitors had a negligible influence on

HR011303 uptake. HR011303 had high permeability and entered the liver and kidney through passive diffusion instead of transporter mediation. Significant active uptake of M5 was observed for OAT3-, OATP1B3-, and OATP1B1-transfected cells, and the ratios of their uptake rates to mock cells were 46.46, 18.98, and 14.21 respectively (Fig. 5). After adding the inhibitors of these transporters, the uptake rates of M5 decreased significantly. Unlike these transporters, only slight or negligible active uptake was observed in OAT1- and OCT2-transfected cells compared with mock cells.

The time-dependent uptake of M5 by OAT3, OATP1B3, and OATP1B1 was measured at a substrate concentration of 5 μM. Uptake was linear with time in the first 2 min of incubation (Fig. 6). OAT3-, OATP1B3-, and OATP1B1-mediated uptakes of M5 were further determined at various substrate concentrations after 2 min of incubation. For OATP1B1, OATP1B3, and OAT3, the uptake of M5 increased with the substrate concentration ranging from 1 μM to 50 μM and reached a plateau at approximately 50 μM for OATP1B3 and 100 μM for OATP1B1 and OAT3 (Fig. 6). The kinetic parameters are presented in Table 1. Only the OATP1B3-mediated uptake of M5 showed apparent substrate inhibition after reaching 50 μM (K_i=252.7 μM).

Stability of M5 in human plasma. HR011303 accounted for 87.9% of the total exposure of drug-related substances, whereas M5 was less than 1% in human plasma samples that mixed according to the AUC pooling principle (Hop et al., 1998). This finding contradicted our result that M5 in the liver was transported to the blood via MRP3. To explain this phenomenon, stability of M5 in human plasma at physiological body temperature was tested, and the results are shown in Fig. 7. After incubation at 37°C for 5 min, the M5 concentration dropped to less than 40% of the initial incubation concentration. And after 20 min, less than 10% of M5 remained in human plasma. The protease inhibitor cocktail significantly improved M5stability.

DMD Fast Forward. Published on December 3, 2021 as DOI: 10.1124/dmd.121.000582
This article has not been copyedited and formatted. The final version may differ from this version.

Hepatobiliary efflux of HR011303. SCRHs were used to study the bile efflux process of drug-related substances of HR011303 after administration. When SCRHs were treated with HR011303 alone, M5, the glucuronide metabolite of HR011303, was the major compound excreted into bile. The BEI value of M5 was 23.44 (Fig. 8). With the addition of MK571, an inhibitor of MRP2/Mrp2, the BEI value decreased to 12.25 (Fig. 8). However, novobiocin (an inhibitor of BCRP) and verapamil (an inhibitor of P-gp) had negligible effects on M5 bile efflux. M5 in rat hepatocytes became an effluent in the bile via MRP2. Based on the rat hepatobiliary efflux results, SCHHs were used to explore bile efflux in humans, and MK571 was used to evaluate the role of MRP2 in the efflux process. Similar to the results in SCRH, both HR011303 and M5 were detected in cells treated with HR011303 alone. However, the BEI values of HR011303 and M5 in SCHH were 7.49% and 4.11%, respectively, and these values were both less than 10%. MK571 inhibited the entry of M5 into bile (Fig. 8). The means of HR011303 and M5 excretion showed significant inter-species differences. HR011303 and M5 were not tend to be excreted into bile in humans, whereas they were transported to bile via Mrp2 in rats.

Efflux transporter MRP2/Mrp2 study. As present in Fig. 9, the ratios of ATP-dependent uptake to the nonspecific adsorption (+ATP/-ATP ratio) of M5 were 33.35 (1 μM) and 15.27 (10 μM) for MRP2. While for Mrp2, the +ATP/-ATP ratios were 18.24 (1 μM) and 6.65 (10 μM). No significant ATP-dependence transport was observed in HR011303 for both MRP2 and Mrp2. Similarly, we conclude that M5 rather than HR011303 was the substrate of MRP2 and Mrp2, which also means M5 produced in hepatocytes can be transported into bile by MRP2/Mrp2.

DMD Fast Forward. Published on December 3, 2021 as DOI: 10.1124/dmd.121.000582
This article has not been copyedited and formatted. The final version may differ from this version.

Discussion

After the oral administration of [^{14}C]HR011303, 87.20% of radioactive substances were excreted in the feces of rats versus 81.50% in human urine, which was completely opposite. Similar phenomena have been reported in previous kinds of literatures. After administration of [^{14}C]fenclofenac, the cumulative radioactivity recovery in feces accounted for 86% in rats. However, in humans, 93% of the radioactive compounds underwent urine excretion. Greeslade proposed that the extreme differences in excretion might be due to the difference in the molecular weight threshold for biliary excretion in diverse species (Greenslade et al., 1980). In addition, it is proposed that the molecular weight cutoffs for anionic compounds were approximately 400 Da in rats and 475 Da in humans. It means that anionic compounds with molecular weight over 400 Da are preferentially excreted in bile in rats (Yang et al., 2009). The results of a study on the excretion of pranoprofen in different species (rats, mice, guinea pigs, and rabbits) indicated that the drug was more likely to be excreted through urine with increasing urine pH level (Arima and Kato, 1990). Bromhexine also showed species differences in terms of excretion in mice, rats, rabbits, dogs, and humans. This phenomena can be explained by the differences in the ability of the species to conjugate basic metabolites (Kopitar et al., 1973). Lesinurad is a first-generation selective URAT1 inhibitor (Hoy, 2016). According to published data, the radioactivity recovery rate shows a discrepancy in excretion between humans and rats. Approximately 75.3% of the radioactivity was excreted in rat feces, whereas 63.4% was excreted in human urine (EMA, 2016; Vishal et al., 2019). The reason for the differences in lesinurad excretion among species is not thoroughly investigated. In the present study, we attempted to explain the species differences in HR011303 excretion. The molecular weight of M5 is 513 Da, which is greater than 475 Da, M5 was effluxed into rat bile and was not well effluxed into

human bile. Moreover, the carboxylic acid moiety of glucuronic acid is ionized at physiological pH and then recognized by the renal organic anion transporter systems in humans, thus enabling glucuronides to be secreted in urine. The pH value of human urine was generally in the range of 4.6–8.4 (Klette et al., 2002), which was not obviously higher than that of rats (6.5–7.0). However, the proportion of HR011303-related compounds excreted in urine still largely differed between rats (10.06%) and humans (81.50%). Therefore, the remarkable difference in mass balance results in rats and humans was not well explained by the molecular weight and pH value. Other factors may be involved in the HR011303 disposition in humans and rats.

After HR011303 into the human body, it was metabolized by UGTs to produce glucuronic acid conjugate M5 in both liver and kidney microsomes (companion manuscript, DMD-AR-2021-000581). Similarly, we studied the metabolic sites of HR011303 in rats. HR011303 can be metabolized to M5 only in the RLMs. M5 could not be generated from HR011303 in the RKMs. HR011303 can be metabolized to M5 in both human and rat hepatocytes, but urine is the major means of excretion way in humans. Thus, M5 or HR011303 in human hepatocytes might have first returned to the blood and then into the kidney. The transport process of HR01103 and M5 from hepatocytes into the blood may exhibit species differences.

Glucuronides can be excreted into bile following their canalicular transport by MRP2 or urine following their sinusoidal transport into the blood by MRP3 (Parkinson et al., 2001). MRP3 is an ATP-dependent, unidirectional efflux pump localized in the basolateral (sinusoidal) membrane. It mediates the efflux of substrates, particularly glucuronides and glutathione conjugates, into sinusoidal blood at the expense of ATP hydrolysis (Borst and Elferink, 2002; Hillgren et al., 2013). Wang quantified and compared a range of hepatic transporters in various species and found that MRP3 expression level in rat liver tissue was much lower than that in

human liver and was even lower than the LLOQ (0.23 fmol) (Wang et al., 2015). Based on this distribution difference, MRP3 might play an important role in the distribution and excretion of HR011303 and its major metabolite M5. HR011303 and M5 efflux were studied in human MRP3-expressing membrane vesicles. As we speculated, M5 rather than HR011303 can be effluxed into the blood via MRP3.

Although M5 is transported into the blood through MRP3, the abundance of M5 in plasma is low. On the one hand, M5 is unstable in plasma at the physiological temperature of the human body (Fig. 6). When M5 is transported from the liver to the blood, most of it is hydrolyzed at 37°C. The sample preparation of quantifying M5 in human plasma by LC-MS/MS needs to be performed on ice water and requires the addition of protease inhibitors in freshly collected plasma before aliquoting. On the other hand, M5 can be taken up by the transporters OATP1B1, OATP1B3, and OAT3. Hence, part of the M5 in blood was taken up into the liver or kidney. All of these factors contributed to the low abundance of M5 in human plasma.

In humans and rats, HR011303 is mostly metabolized to M5 in the liver. In human liver, the formed M5 is effluxed into the blood by MRP3. By contrast, in rat liver, M5 is excreted into bile. Transporters on the bile duct side may be involved in this process. Humans are poorer biliary excreters compared with rats (Mahmood and Sahajwalla, 2002). The elimination rates of MRP2/Mrp2 specific substrates in isolated rat liver cells were 4–6 times faster than in human hepatocytes(Li et al., 2008). The amount of MRP2/Mrp2 in rat liver was approximately 10 times higher than those of other species, including humans. (Li et al., 2009). We used SCRH and SCHH to study the bile efflux of drug-related substances after administration of HR011303. Transporter inhibitors were used to explore the contribution of different transporters to the efflux process. In rats, HR011303 was metabolized to M5 in the liver and excreted as M5 into bile. In

contrast, HR011303 and M5 did not show any tendency to be effluxed into bile in humans. The addition of MK571 (an inhibitor of Mrp2) can significantly inhibited the bile efflux of M5 in rats. Mrp2 may be the main transporters involved in the efflux of M5 into bile in rats. Considering the totally different distribution of MRP2/Mrp2 and MRP3/Mrp3 in human and rat hepatocytes and their respective roles in drug disposition, we proposed that the competition for M5 between MRP2/Mrp2 and MRP3/Mrp3 leads to a reverse excretion pathway in humans and rats.

By using human MRP2 and rat Mrp2-expressing membrane vesicles, we came to the conclusion that M5 was the substrate of both MRP2 and Mrp2. Combining that MRP2/Mrp2 expression level in rat liver is about 10 times of human, we speculate that M5 in rat liver is mainly excreted into bile through Mrp2. While in human hepatocytes, we conjecture that MRP3 performs better than MRP2 in the competitive transport of M5.

This study investigated the key transporters responsible for the species differences in HR011303 excretion and explored the reasons for the low plasma exposure of the main metabolite M5. The metabolism and distribution process after the oral administration of HR011303 in humans and rats are shown in Figs. 10 and 11. In humans, HR011303 enters into the liver and kidney through passive diffusion and is metabolized by UGTs to produce the major metabolite M5. The majority of M5 produced in the liver is effluxed into the blood by MRP3 and then enters the kidney as M5 or HR011303. In rats, HR011303 is metabolized in the liver to the main metabolite M5, which is then excreted into bile by Mrp2 and undergoes further metabolism in the gut before excretion in the feces.

DMD Fast Forward. Published on December 3, 2021 as DOI: 10.1124/dmd.121.000582
This article has not been copyedited and formatted. The final version may differ from this version.

Conflict of Interest

G.Z.L. and Q.H. are the employees of Jiangsu hengrui medicine Co., Ltd. and the other authors declare that they have no competing interest.

Authorship contribution

Participated in research design: Diao, Chen XY, Guo, Liu, Li, Huang, Zhong, Yu

Conducted experiments: Liu, Guo, Meng, Xue

Performed data analysis: Liu, Guo, Xue, Chen ZD, Wu, Diao

Wrote or contributed to the writing of the manuscript: Liu, Guo, Diao, Chen XY, Zheng, Wu

References

Ansede JH, Smith WR, Perry CH, St. Claire RL, and Brouwer KR (2010) An in vitro assay to assess transporter-based cholestatic hepatotoxicity using sandwich-cultured rat hepatocytes. *Drug Metab Dispos* **38:**276-280.

Arima N and Kato Y (1990) Species differences in absorption, metabolism and excretion of pranoprofen, a 2-arylpropionic acid derivative, in experimental animals. *J Pharmacobiodyn* **13:**739-744.

Borst P and Elferink RO (2002) Mammalian ABC transporters in health and disease. *Annu Rev Biochem* **71:**537-592.

Chandra P and Brouwer KLR (2004) The complexities of hepatic drug transport: current knowledge and emerging concepts. *Pharm Res* **21:**719-735.

Chandra P, Johnson BM, Zhang P, Pollack GM, and Brouwer KLR (2005) Modulation of hepatic canalicular or basolateral transport proteins alters hepatobiliary disposition of a model organic anion in the isolated perfused rat liver. *Drug Metab Dispos* **33:**1238-1243.

EMA (2016) International non-proprietary name: Lesinurad. *European Medicines Agency* **EMEA/H/C/003932/0000:**128.

Gao C, Zhang H, Guo Z, You T, Chen X, and Zhong D (2012) Mechanistic studies on the absorption and disposition of scutellarin in humans: Selective OATP2B1-mediated hepatic uptake is a likely key determinant for its unique pharmacokinetic characteristics. *Drug Metab Dispos* **40:**2009-2020.

Greenslade D, Havler ME, Humphrey MJ, Jordan BJ, and Rance MJ (1980) Species differences in the metabolism and excretion of fenclofenac. *Xenobiotica* **10:**753-760.

Grime K and Paine SW (2013) Species differences in biliary clearance and possible relevance of hepatic uptake and efflux transporters involvement. *Drug Metab Dispos* **41:**372-378.

Hillgren KM, Keppler D, Zur AA, Giacomini KM, Stieger B, Cass CE, and Zhang L (2013) Emerging transporters of clinical importance: an update from the international transporter consortium. *Clin Pharmacol Ther* **94:**52-63.

Hop CECA, Zhen W, Chen Q, and Kwei G (1998) Plasma-pooling methods to increase throughput for in vivo pharmacokinetic screening. *J Pharm Sci* **87:**901-903.

Hoy SM (2016) Lesinurad: First global approval. *Drugs* **76:**509-516.

Jiang J, Pang X, Dai X, Diao X, Chen X, Zhong D, Chen Y, Li L, and Wang Y (2016) Effect of N-methyl deuteration on metabolism and pharmacokinetics of enzalutamide. *Drug Des Devel Ther* **10:**2181-2191.

Klette KL, Horn CK, Stout PR, and Anderson CJ (2002) LC-MS analysis of human urine specimens for 2-Oxo-3-Hydroxy LSD: method validation for potential interferants and stability study of 2-Oxo-3-Hydroxy LSD under various storage conditions. *J Anal Toxicol* **26:**193-200.

Konig J, Muller F, and Fromm MF (2013) Transporters and drug-drug interactions: Important determinants of drug disposition and effects. *Pharmacol Rev* **65:**944-966.

Kopitar Z, Jauch R, Hankwitz R, and Pelzer H (1973) Species differences in metabolism and excretion of bromhexine in mice, rats, rabbits, dogs and man. *Eur J Pharmacol* **21:**6-10.

Li M, Yuan HD, Li N, Song GT, Zheng Y, Baratta M, Hua F, Thurston A, Wang J, and Lai Y (2008) Identification of interspecies difference in efflux transporters of hepatocytes from dog, rat, monkey and human. *Eur J Pharm Sci* **35:**114-126.

Li N, Zhang Y, Hua F, and Lai Y (2009) Absolute difference of hepatobiliary transporter multidrug resistance-associated protein (MRP2/Mrp2) in liver tissues and isolated hepatocytes from rat, dog, monkey, and human. *Drug Metab Dispos* **37:**66-73.

Lin JH, Chiba M, Balani SK, Chen IW, Kwei GY, Vastag KJ, and Nishime JA (1996) Species differences in the pharmacokinetics and metabolism of indinavir, a potent human immunodeficiency virus protease inhibitor. *Drug Metab Dispos* **24:**1111-1120.

Ma L, Zhao L, Hu H, Qin Y, Bian Y, Jiang H, Zhou H, Yu L, and Zeng S (2014) Interaction of five anthraquinones from rhubarb with human organic anion transporter 1 (SLC22A6) and 3 (SLC22A8) and drug-drug interaction in rats. *J Ethnopharmacol* **153:**864-871.

Mahmood I and Sahajwalla C (2002) Interspecies scaling of biliary excreted drugs. *J Pharm Sci* **91:**1908-1914.

Mazur CS, Kenneke JF, Hess-Wilson JK, and Lipscomb JC (2010) Differences between human and rat intestinal and hepatic bisphenol a glucuronidation and the influence of alamethicin on in vitro kinetic measurements. *Drug Metab Dispos* **38:**2232-2238.

Nezasa KI, Tian XB, Zamek Gliszczynski MJ, Patel NJ, Raub TJ, and Brouwer KLR (2006) Altered hepatobiliary disposition of 5 (and 6)-carboxy-2′,7′-dichlorofluorescein in Abcg2 (Bcrp1) and Abcc2 (Mrp2) konckout mice. *Drug Metab Dispos* **34:**718-723.

Nigam and Sanjay K (2015) What do drug transporters really do? *Nat Rev Drug Discov* **14:**29-44.

Pan GY, Boiselle C, and Wang JL (2012) Assessment of biliary clearance in early drug discovery using sandwich‐cultured hepatocyte model. *J Pharm Sci* **101:**1898-1908.

Parkinson A, Ogilvie BW, Buckley DB, Kazmi F, and Parkinson O (2001) Biotransformation of xenobiotics. *Casarett and Doull's Toxicology: The Basic Science of Poisons*.

Peng JB, Hu QY, Gu CY, Liu BN, Jin FF, Yuan JJ, Feng J, Zhang L, Lan J, Dong Q, and Cao GQ (2016) Discovery of potent and orally bioavailable inhibitors of human uric acid transporter 1 (hURAT1) and binding mode prediction using homology model. *Bioorg Med Chem Lett* **26:**277-282.

Ratzan KR, Baker HB, and Lauredo I (1978) Excretion of Cefamandole, Cefazolin, and Cephalothin into T-Tube Bile. *Antimicrob Agents Chemother* **13:**985-987.

Robertson EE and Rankin GO (2006) Human renal organic anion transporters: Characteristics and contributions to drug and drug metabolite excretion. *Pharmacol Ther* **109:**399-412.

Shen GL, Zhuang XM, Yuan M, Sun HX, and Li H (2012) Evaluation of P-glycoprotein mediated in vitro loperamide biliary excretion with sandwich-cultured rat hepatocytes model. *Acta Pharmaceutica Sinica* **47:**459-465.

Shiratani H, Katoh M, Nakajima M, and Yokoi T (2008) Species differences in UDP-glucuronosyltransferase activities in mice and rats. *Drug Metab Dispos* **36:**1745-1752.

Stringer RA, Strain-Damerell C, Nicklin P, and Houston JB (2009) Evaluation of recombinant cytochrome P450 enzymes as an in vitro system for metabolic clearance predictions. *Drug Metab Dispos* **37:**1025-1034.

Takano R, Murayama N, Horiuchi K, Kitajima M, Kumamoto M, Shono F, and Yamazaki H (2010) Blood concentrations of acrylonitrile in humans after oral administration extrapolated from in vivo rat pharmacokinetics, in vitro human metabolism, and physiologically based pharmacokinetic modeling. *Regul Toxicol Pharmacol* **58:**252-258.

Takeuchi R, Shinozaki K, Nakanishi T, and Tamai I (2015) Local drug-drug interaction of donepezil with cilostazol at breast cancer resistance protein (ABCG2) increases drug accumulation in heart. *Drug Metab Dispos* **44:**68-74.

Tu MJ, Sun SY, Wang K, Peng XY, Wang RH, Li LP, Zeng S, Zhou H, and Jiang HD (2013) Organic cation transporter 1 mediates the uptake of monocrotaline and plays an important role in its hepatotoxicity. *Toxicology* **311:**225-230.

Van De Wetering K, Zelcer N, Kuil A, Feddema W, Hillebrand M, Vlaming MLH, Schinkel AH, Beijnen JH, and Borst P (2007) Multidrug resistance proteins 2 and 3 provide alternative routes for hepatic excretion of morphine-glucuronides. *Mol Pharmacol* **72:**387-394.

Vishal S, Yang C, Shen ZC, Kerr BM, Tieu K, Wilson DM, Hall J, Gillen M, and Lee CA (2019) Metabolism and disposition of lesinurad, a uric acid reabsorption inhibitor, in humans. *Xenobiotica* **49:**811-822.

Vlaming MLH, Mohrmann K, Wagenaar E, De Waart DR, Elferink RPJO, Lagas JS, Van Tellingen O, Vainchtein LD, Rosing H, Beijnen JH, Schellens JHM, and Schinkel AH (2006) Carcinogen and anticancer drug transport by Mrp2 in vivo: Studies using Mrp2(Abcc2) knockout mice. *J Pharmacol Exp Ther* **318:**319-327.

Wang J, Yao W, Fan D, Qiu ZJ, Song JQ, Pan K, and Hang TJ (2019) An LC–MS/MS method for quantification of HR011303, a novel highly selective urate transporter 1 inhibitor in beagle dogs and the application to a pharmacokinetic study. *Biomed Chromatogr* **33:**1-7.

Wang L, Prasad B, Salphati L, Chu XY, Gupta A, Hop CECA, Evers R, and Unadkat JD (2015) Interspecies variability in expression of hepatobiliary transporters across human, dog, monkey, and rat as determined by quantitative proteomics. *Drug Metab Dispos* **43:**367-374.

Xue YR, Yao S, Liu Q, Peng ZL, Deng QQ, Liu B, Ma ZH, Wang L, Zhou H, Ye Y, and Pan GY (2020) Dihydro-stilbene gigantol relieves CCl4-induced hepatic oxidative stress and

inflammation in mice via inhibiting C5b-9 formation in the liver. *Acta Pharmacol Sin* **41:**1433-1445.

Yang XN, Gandhi YA, Duignan DB, and Morris ME (2009) Prediction of biliary excretion in rats and humans using molecular weight and quantitative structure-pharmacokinetic relationships. *The AAPS Journal* **11:**511-525.

Footnote

This research was financially supported by a grant from the National Natural Science Foundation of China [81903701]

DMD Fast Forward. Published on December 3, 2021 as DOI: 10.1124/dmd.121.000582
This article has not been copyedited and formatted. The final version may differ from this version.

Legend to Figures

Figure 1. Cumulative radioactivity recovery of rats and humans. A, cumulative recovery in rat urine and feces within 0–168 h. B, cumulative recovery in rat bile within 48 h. C, cumulative recovery in human urine and feces. Data were expressed as mean ± S.D. (n=6).

Figure 2. Structure and abundance of major metabolites of HR011303 in rats (A) and humans (B). Metabolites that were less than 4% of the dose were not presented. *multiple isomers.

Figure 3. Relative amounts of HR011303 and M5 after HR011303 was incubated with human (A) and rat microsomes (B) (n=2).

Figure 4. Direct transport of HR011303 and M5 by MRP3. HR011303 or M5 was incubated with MRP3-expressing membrane vesicle with or without the presence of ATP for 10 min. Data were expressed as mean + S.D. (n=3).

Figure 5. Uptake of M5 in the OATP1-, OATP1B3-, OATP2B1-, OAT1, OAT3, or OAT3-transfected HEK293 cells. Incubation concentration was 5 μM and the uptake time was 10 min for all cells. Data were expressed as mean + S.D. (n=3).

Figure 6. The time dependence of M5 in HEK-mock and HEK-OATP1B1 (A), OATP1B3 (B) and OAT3 (C) at an incubation concentration of 5 μM. The active uptake kinetic curves of M5 by OATP1B1 (D), OATP1B3 (E) and OAT3 (F) at an incubation time of 2 min. Data were expressed as mean ± S.D. (n=3).

Figure 7. Relative remaining of M5 (initial concentration: 5 μM) in human plasma after incubation for up to 40 min (n=2).

Figure 8. Accumulation of HR011303 in SCRH (A) and SCHH (C) as well as the accumulation of M5 in SCRH (B) and SCHH (D) with or without Ca^{2+} after treatment with HR011303 alone. The calculated BEI value was marked on the corresponding column. Data were expressed as mean + S.D. (n=3), **, $P<0.005$, ***, $P<0.001$.

DMD Fast Forward. Published on December 3, 2021 as DOI: 10.1124/dmd.121.000582
This article has not been copyedited and formatted. The final version may differ from this version.

Figure 9. Direct transport of HR011303 and M5 by MRP2 (A) and Mrp2 (B). HR011303 or M5 was incubated with MRP2 and Mrp2-expressing membrane vesicle with or without the presence of ATP for 10 min. Data were expressed as mean + S.D. (n=3).

Figure 10. Proposed scheme of the disposition and excretion processes of HR011303 and M5 in human. The width of the arrows represents the relative amount of substrate undergoing a certain process.

Figure 11. Proposed scheme of the disposition and excretion processes of HR011303 and M5 in rats. The width of the arrows represents the relative amount of substrate undergoing a certain process.

DMD Fast Forward. Published on December 3, 2021 as DOI: 10.1124/dmd.121.000582
This article has not been copyedited and formatted. The final version may differ from this version.

Table 1 Main kinetic parameters for the transportation of M5 in HEK-OATP1B1, OATP1B3 and OAT3 cell lines.

	K_m (μM)	V_{max} (pmol/min/mg protein)	K_i (μM)	V_{max}/K_m (μL/min/mg protein)
OATP1B1	32.00 ± 6.72	168.9 ± 11.75	-	5.28
OATP1B3	25.84 ± 13.66	376.8 ± 115.5	252.8 ± 242.6	14.58
OAT3	12.15 ± 3.32	318.0 ± 22.2	-	26.17

DMD Fast Forward. Published on December 3, 2021 as DOI: 10.1124/dmd.121.000582
This article has not been copyedited and formatted. The final version may differ from this version.

Figure 1

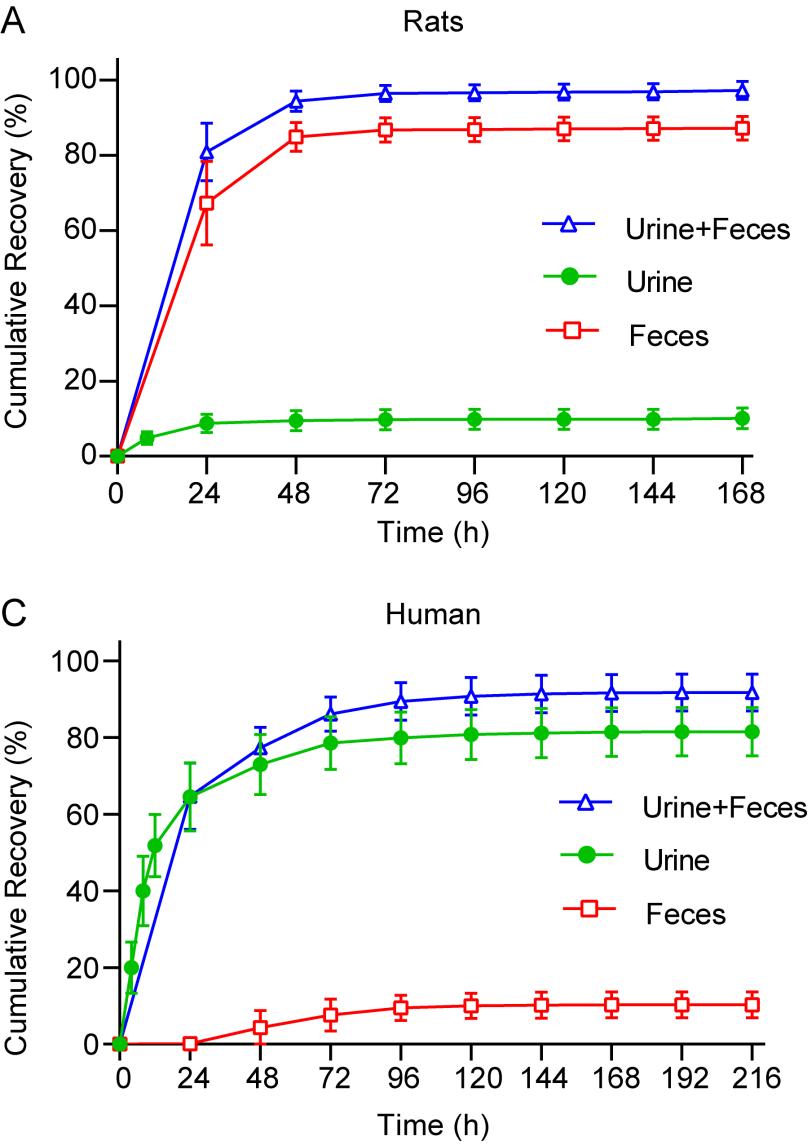

DMD Fast Forward. Published on December 3, 2021 as DOI: 10.1124/dmd.121.000582
This article has not been copyedited and formatted. The final version may differ from this version.

Figure 2

A

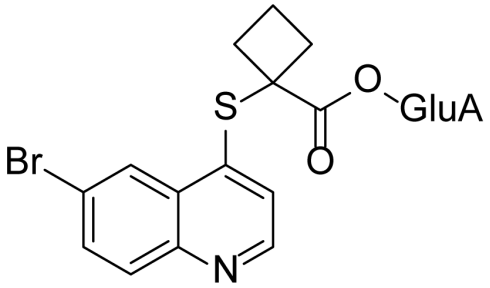

M5*

Bile: 27.58% of dose

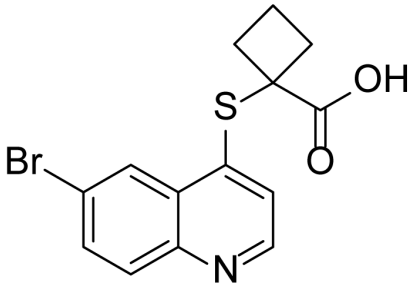

HR011303

Plasma: 97% of AUC
Bile: 38.64% of dose
Feces: 43.08% of dose

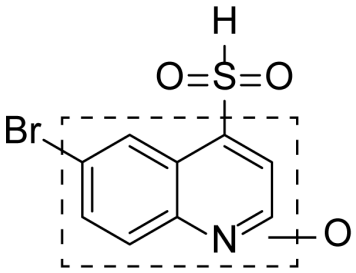

M6

Urine: 9.09% of dose
Feces: 39.76% of dose

B

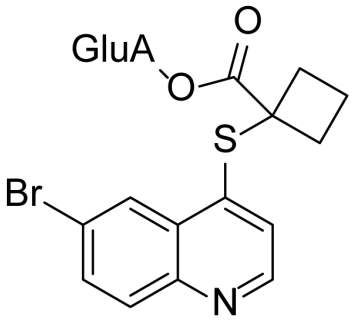

M5

Urine: 51.57% of dose

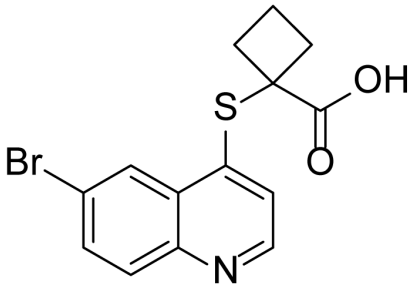

HR011303

Plasma: 87.93% of AUC
Urine: 4.62% of dose
Feces: 4.24% of dose

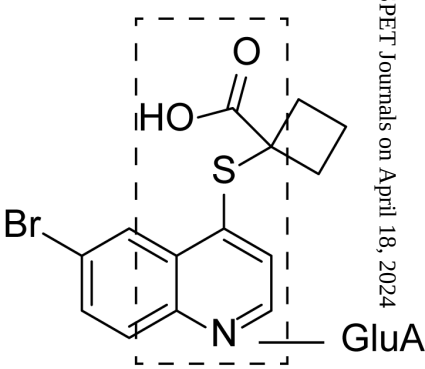

M5/2

Urine: 18.06% of dose

DMD Fast Forward. Published on December 3, 2021 as DOI: 10.1124/dmd.121.000582
This article has not been copyedited and formatted. The final version may differ from this version.

Figure 3

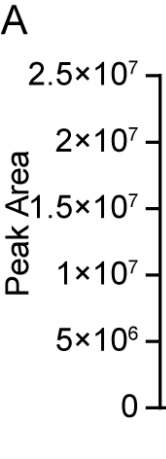

DMD Fast Forward. Published on December 3, 2021 as DOI: 10.1124/dmd.121.000582
This article has not been copyedited and formatted. The final version may differ from this version.

Figure 4

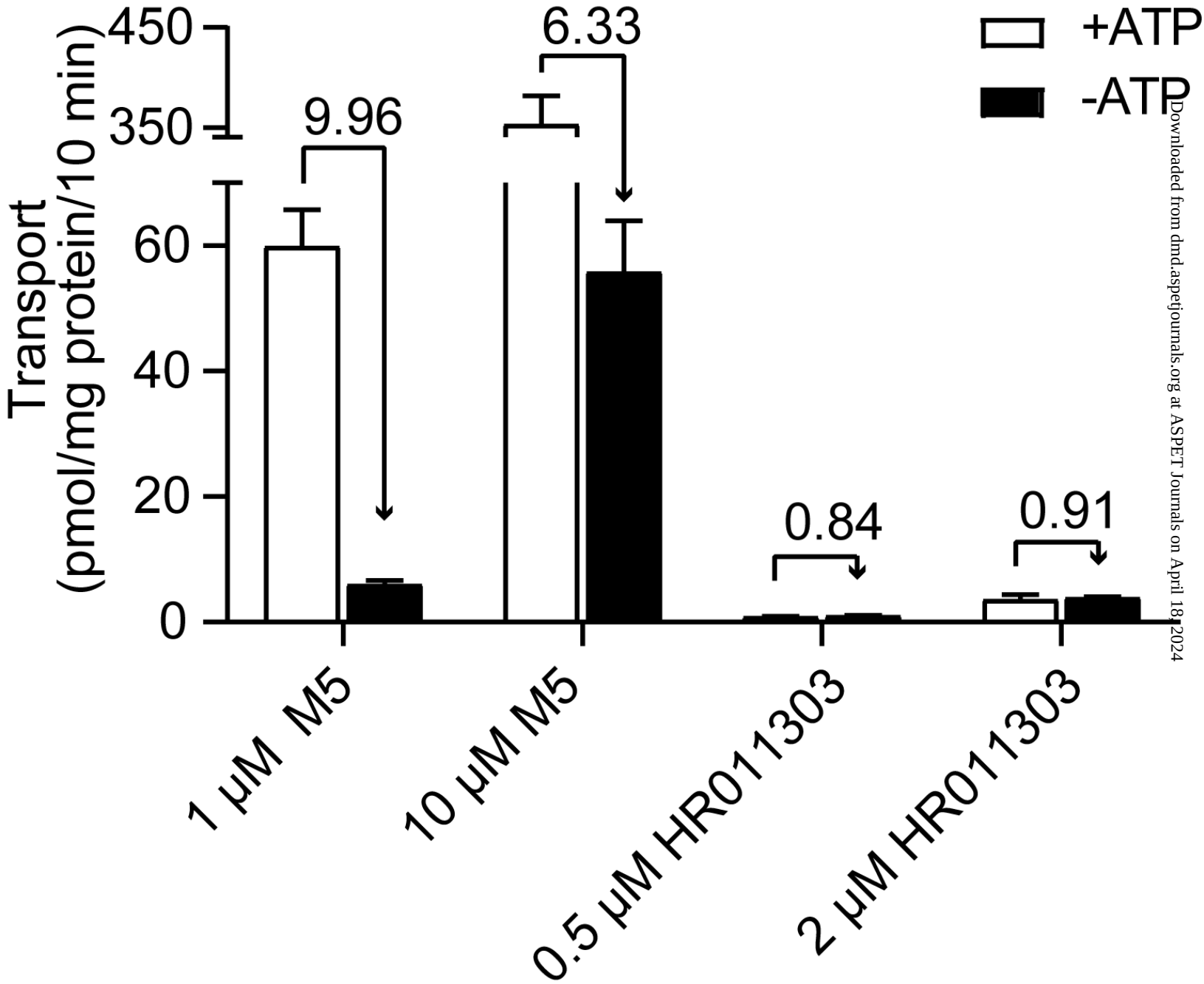

DMD Fast Forward. Published on December 3, 2021 as DOI: 10.1124/dmd.121.000582
This article has not been copyedited and formatted. The final version may differ from this version.

Figure 5

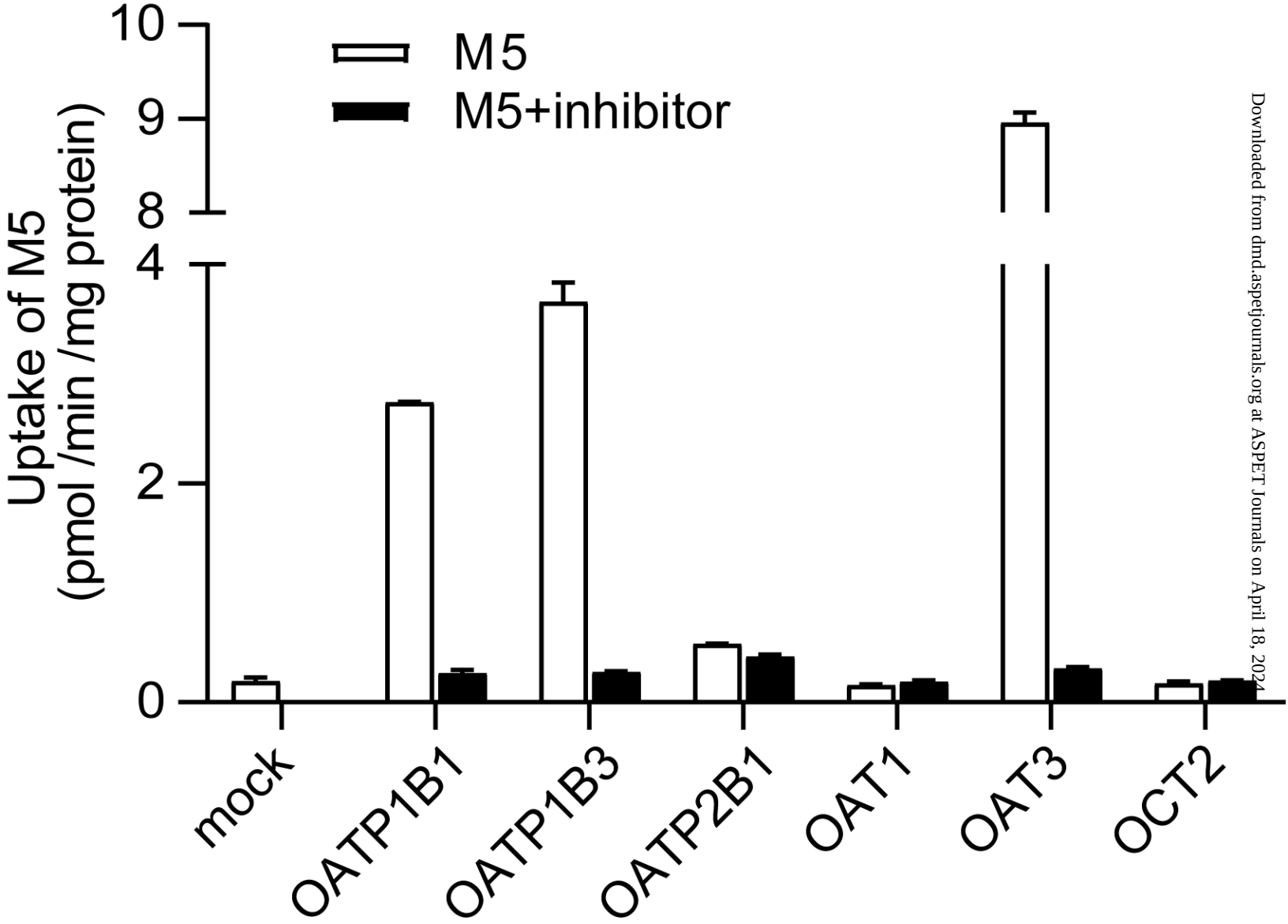

DMD Fast Forward. Published on December 3, 2021 as DOI: 10.1124/dmd.121.000582
This article has not been copyedited and formatted. The final version may differ from this version.

Figure 6

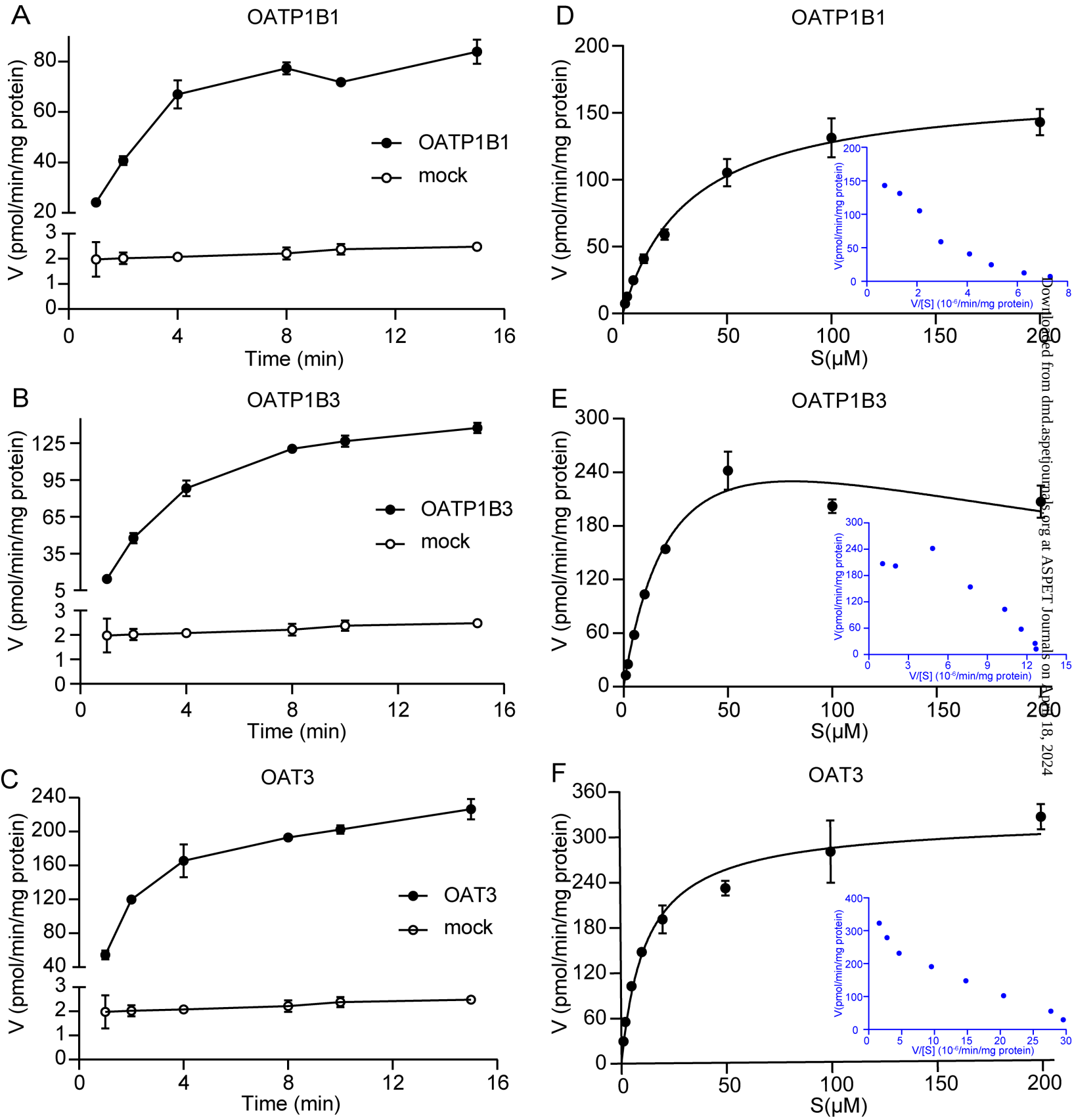

DMD Fast Forward. Published on December 3, 2021 as DOI: 10.1124/dmd.121.000582
This article has not been copyedited and formatted. The final version may differ from this version.

Figure 7

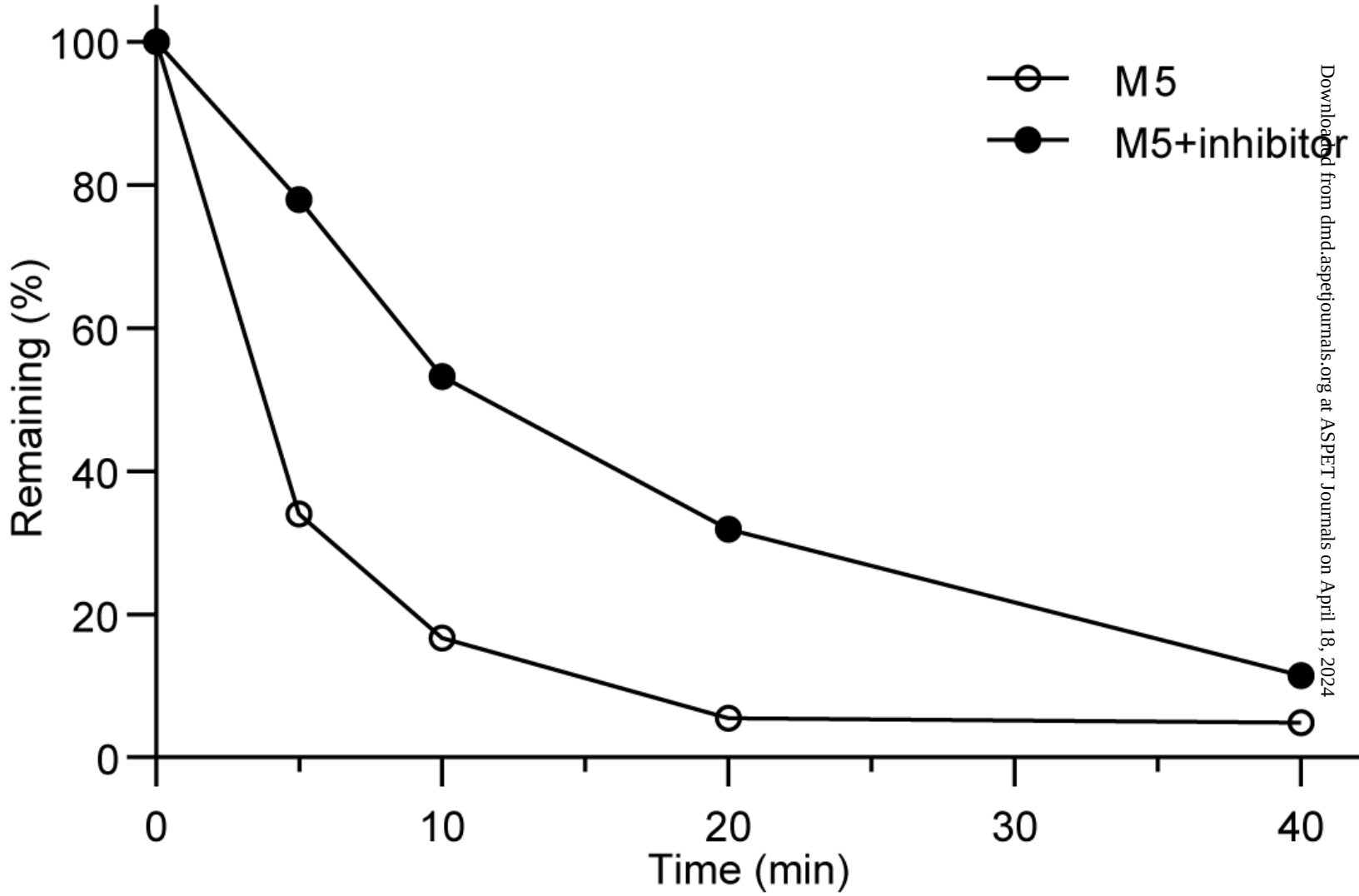

DMD Fast Forward. Published on December 3, 2021 as DOI: 10.1124/dmd.121.000582
This article has not been copyedited and formatted. The final version may differ from this version.

Figure 8

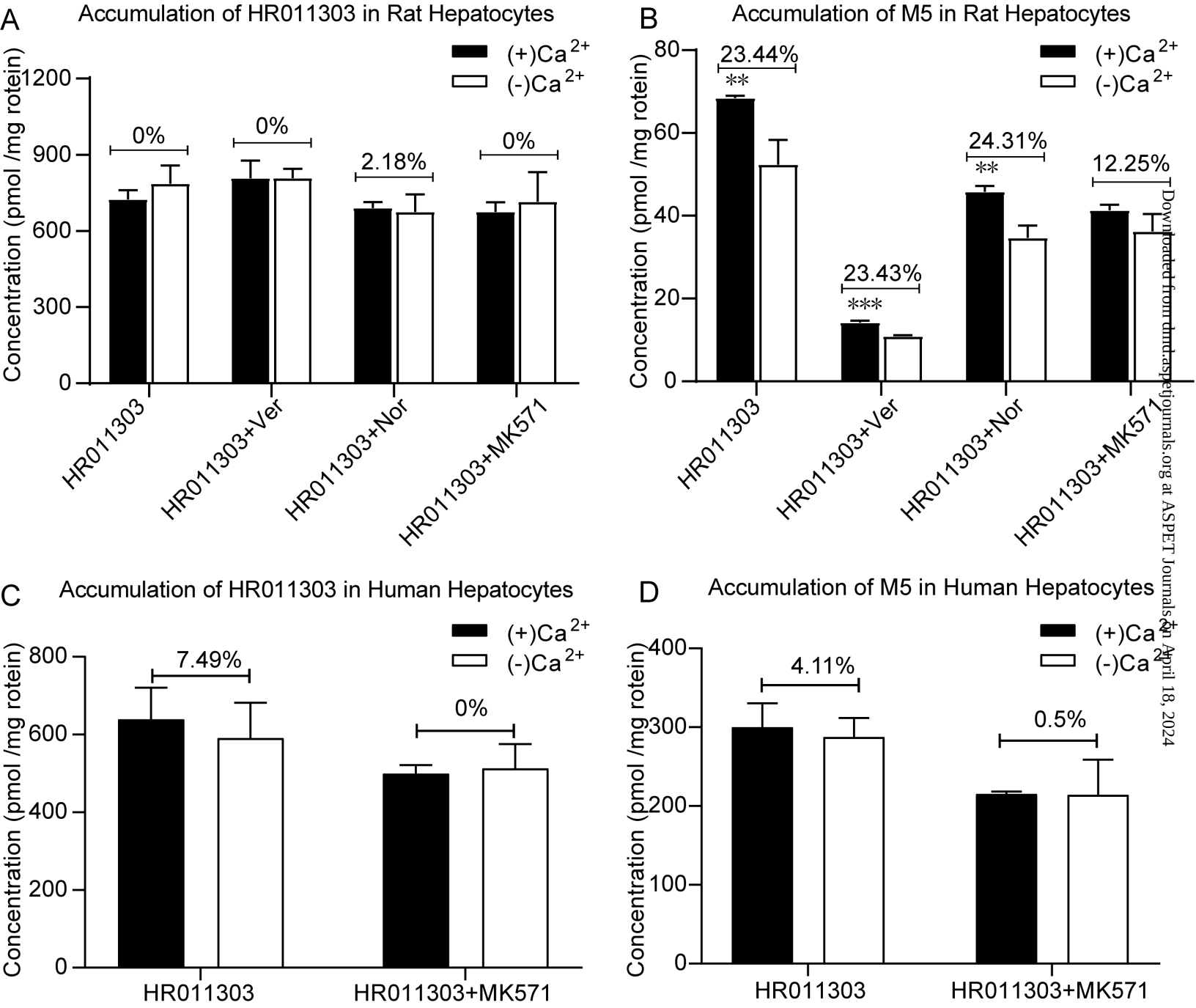

DMD Fast Forward. Published on December 3, 2021 as DOI: 10.1124/dmd.121.000582
This article has not been copyedited and formatted. The final version may differ from this version.

Figure 9

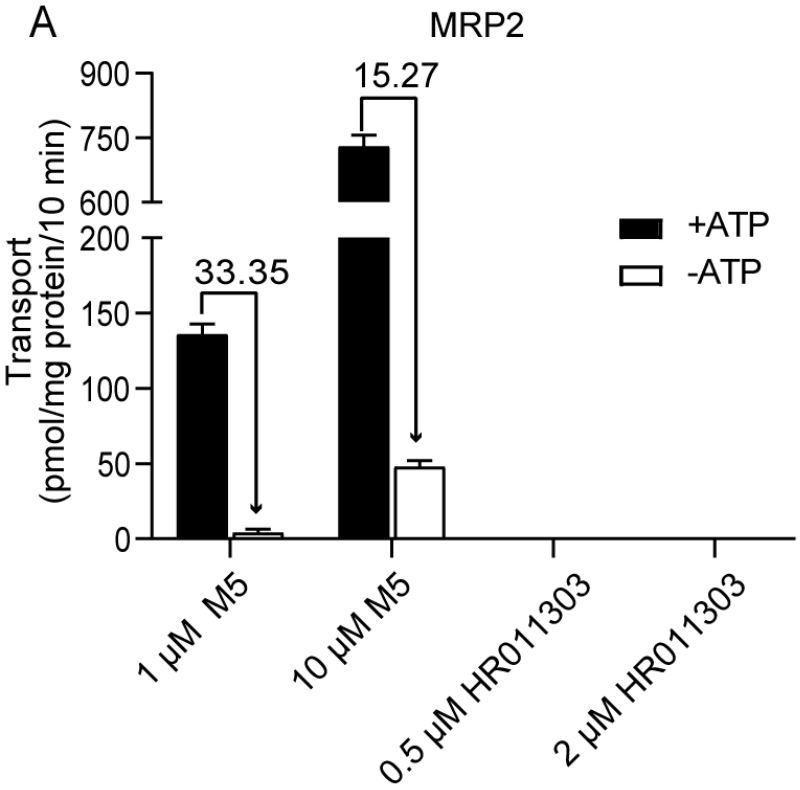

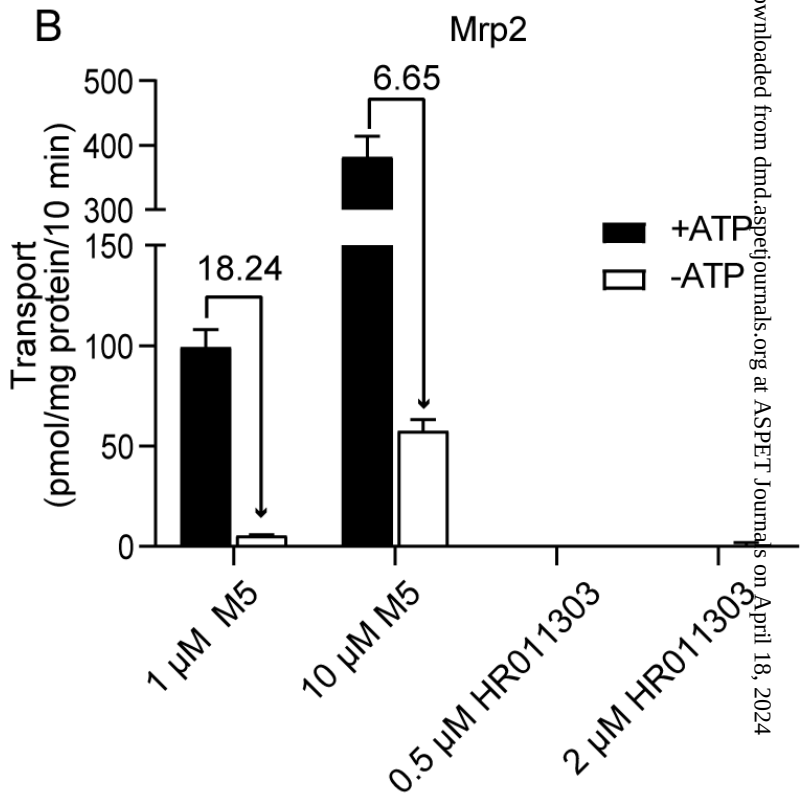

DMD Fast Forward. Published on December 3, 2021 as DOI: 10.1124/dmd.121.000582
This article has not been copyedited and formatted. The final version may differ from this version.

Figure 10

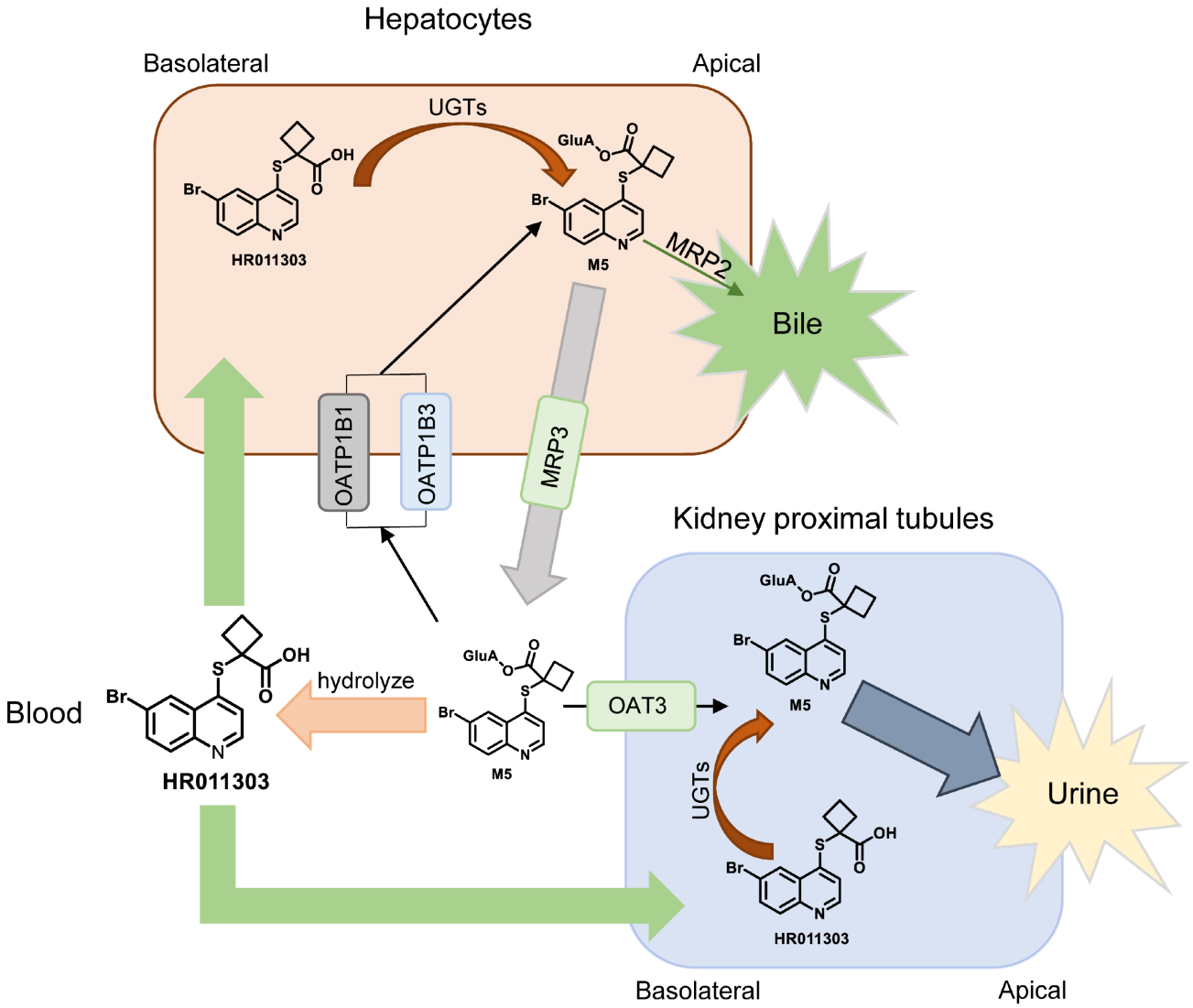

DMD Fast Forward. Published on December 3, 2021 as DOI: 10.1124/dmd.121.000582
This article has not been copyedited and formatted. The final version may differ from this version.

Figure 11